

Metal ion coordination in ‘R’ and ‘T’ state hybrid hemoglobins as revealed by optical, EPR and sulphhydryl reactivity studies

S RAMASAMY¹, SWARNALATHA VENKATESHRAO¹, J M RIFKIND² and P T MANOHARAN^{1*}

¹Department of Chemistry and Regional Sophisticated Instrumentation Centre, Indian Institute of Technology – Madras, Chennai 600 036, India

²Molecular Dynamics Section, National Institute on Aging, National Institutes of Health, 5600 Nathan Shock Drive, Baltimore, MD 21224, USA
e-mail: ptm@rsic.iitm.ernet.in

Abstract. The sulphhydryl environment in various mixed-metal hybrid hemoglobins, viz. $\mathbf{a}_2(\text{Cu})\text{-}\mathbf{b}_2(\text{FeCO})$, $\mathbf{a}_2(\text{FeCO})\text{-}\mathbf{b}_2(\text{Cu})$, $\mathbf{a}_2(\text{Cu})\text{-}\mathbf{b}_2(\text{Ni})$, $\mathbf{a}_2(\text{Ni})\text{-}\mathbf{b}_2(\text{Cu})$, was studied by reacting them with the sulphhydryl reagent, 4,4'-dithiodipyridine (4-PDS). The reactivity was compared with that of HbCO, NiHb and CuHb. It is found that there exists a correlation between conformational change and metal ion environment, not only at the extreme R and T states but also the intermediate conformations. EPR examinations of these hybrids show that both in *R state*-[Cu(II)-Fe(II)] and *T state*-[Cu(II)-Ni(II)] hybrids at neutral pH and in the absence of IHP, CuPPIX, irrespective of the subunit in which it is present, has a mixed-metal ion environment: Species 1, a five-coordinated Cu^{2+} complex with strong proximal histidine bond and species 2, a four-coordinated complex without any covalent linkage with Ne F8-histidine.

Keywords. Hybrid hemoglobin; –SH reactivity study; EPR; subunit heterogeneity.

1. Introduction

Hemoglobin (Hb) is one of the most representatives of allosteric proteins. The oxygenation process involves 10 partially ligated species including the extreme states – the deoxy Hb (T) and oxy Hb (R)¹. Since oxygen moves from one site to other with great lability, the isolation and study of each partially oxygenated tetramer has not been possible and, for the same reason, the mechanism of cooperative oxygenation is not fully understood. A complete understanding of cooperative behaviour of Hb requires clear knowledge of the tertiary and quaternary structures of the partially ligated species. Different kinds of hybrid Hbs, for example, valency hybrid Hb², mixed-metal hybrid Hb³, intersubunit cross-linked hybrid Hbs,^{4,5} which were regarded as models for the intermediate species, have been investigated so far to gain information about the structural aspects of the intermediates. Among these hybrid Hbs, mixed-metal hybrids having an oxy/carbon monooxy/deoxygenated iron (II) porphyrin in either the *a* (or) *b*-subunit, with the

other subunit having a heterometallated porphyrin in +2 oxidation state can be regarded as good models for testing the properties of intermediates. A variety of mixed-metal hybrid Hbs have been studied so far, which include Co(II)–Fe(II), Ni(II)–Fe(II), Zn(II)–Fe(II), Mn(II)–Fe(II), Cu(II)–Fe(II) hybrid Hbs.

Perutz proposed that the equilibrium between the two quaternary structures depends on the distance between Ne (His–F8) and the plane of the porphyrin.⁶ The T structure is more stable when both the iron atom and the proximal His–F8 are displaced from the porphyrin plane. The stronger bonds between the subunits in the T structure might pull the proximal His–F8 away from the porphyrin plane and thus stretch the Fe–Ne (His–F8) bond. It was concluded by Perutz⁶ that the high spin of the ferrous atom and the associated increase in the bond lengths are the principal causes for the low oxygen affinity of the deoxy quaternary structure. The stabilization of the T structure due to an increase in the Fe–Ne (His–F8) bond distance was a major effect observed only in the *a*-subunits; whereas such stabilization in the *b*-subunit was very small. This difference between the two subunits, the so-called subunit heterogeneity or subunit inequivalence, was first identified by Perutz and co-workers from a variety of measurements on

Dedicated to the memory of the late Professor Bhaskar G Maiya

*For correspondence

Abbreviations: DTT – dithiothreitol; EPR – electron paramagnetic resonance; Hb – hemoglobin; 4-PDS – 4,4'-dithiodipyridine

normal, modified and abnormal Hbs.⁶⁻⁸ In situations like low pH (pH \approx 6.5) or in the presence of inositol-hexaphosphate (IHP), the globin exerts a much larger strain on the Fe(II)–Ne (His–F8) bond in the **a**-subunit than in the **b**-subunit and as a result there is a rupture of this bond in the **a**-subunit. A variety of studies which were done in mixed-metal hybrid Hbs and also in other hybrids, viz., EPR,³ NMR,⁹ transient Raman¹⁰ and oxygen binding studies on Co(II)–Fe(II) hybrid Hbs.¹⁰ Optical, oxygen binding and NMR studies on Ni(II)–Fe(II) hybrid Hbs,^{11,12} NMR on Ru(II)–Fe(II),¹³ resonance Raman studies on valency hybrid Hbs,¹⁴ EPR studies on nitrosyl Hb¹⁵ confirmed the presence of subunit heterogeneity. All these studies were done with the Fe–Ne (His–F8) bond distance as the major consideration, since the existence of this bond plays a definite role in stabilizing the R structure. The results from all these studies were that at pH 7.4, M²⁺ in the **a**-subunit is exclusively 4-coordinate without any covalent linkage with Ne (His–F8), whereas that in **b**-subunit it is exclusively 5-coordinate with an M²⁺–Ne (His–F8) bond. Mixed-metal ion coordination, namely 4- and 5-coordination in copper and nickel-reconstituted Hbs were confirmed by employing electron paramagnetic resonance^{16,17} and resonance Raman¹⁸ techniques respectively. Identification of the presence of two different metal ion environments in CuHb was later extended to the mixed-metal hybrid, [Cu(II)–Fe(II)]¹⁹, and based on their X-band EPR measurements, it was concluded that the 5- and 4-coordination complexes in CuHb are localized in **b** and **a**-subunits respectively.

Now an important question that arises is whether the presence of two different metal ion environments is due to subunit heterogeneity or due to their simultaneous presence in both **a**- and **b**-subunits. In other words, whether an increase in bond distance or cleavage of the M²⁺–Ne (His–F8) bond which leads to stabilization of the T structure is achieved in the **a** subunit alone or also in the **b**-subunit. Explicitly, whether the two different metal ion coordinations, 4- and 5-, are localized in **a** and **b**-subunits respectively, or are present in both subunits in different proportions.

This paper tries to find a suitable answer by employing Q-band EPR spectroscopy for several Cu-containing hybrid Hbs both in R as well as in T state conformations. We have prepared Cu(II)–Fe(II) and Cu(II)–Ni(II) mixed-metal hybrid hemoglobins in which heme in either **a** (or) **b**-subunits are substi-

tuted with Cu(II)PPIX or Ni(II)PPIX and studied the sulphhydryl environment by the use of sulphhydryl reagent 4-PDS and heme environment by employing EPR spectroscopy. The advantage of using **a**₂(Cu)–**b**₂(FeCO) and **a**₂(FeCO)–**b**₂(Cu) hybrid Hbs is that one can obtain half-liganded Hb with all porphyrin metals in +2 valence state and the metal ion in the **a** and the **b**-subunits can be looked into separately by means of EPR spectroscopy; whereas the other set of hybrid Hbs **a**₂(Cu)–**b**₂(Ni) and **a**₂(Ni)–**b**₂(Cu) are representatives of T-state conformations. Earlier X-band EPR investigation on **a**₂(Cu)–**b**₂(FeCO) and **a**₂(FeCO)–**b**₂(Cu) hybrid Hbs¹⁹ revealed the existence of subunit heterogeneity; but these results should be carefully analysed because in X-band studies, the parallel and the perpendicular features merge, making the analysis complex. So we have attempted to separate out the parallel and the perpendicular features by carrying out the EPR measurements at higher frequency to remove possible uncertainties.

2. Experimental section

2.1 Preparation of hybrid Hbs

Nickel (II) protoporphyrin IX (NiPPIX) and copper (II) protoporphyrin IX (CuPPIX) were synthesized according to the methods of Shibayama *et al.*^{19,20} The preparation of Cu(II)–Fe(II) hybrid Hbs were achieved by a slight modification of the reported procedure.¹⁹ HbA₀ was prepared in carbonmonoxy form as described by Kilmartin *et al.*²¹ Separation of **a** and **b** chains from HbA₀ was followed by the procedure of Geraci *et al.*²² Heme-globin separation was carried out by following Rossi–Farelli's acid acetone method.²³ Preparation of CuPPIX or NiPPIX reconstituted chains were done as reported by Shibayama *et al.*^{19,20} Metal reconstituted chains in borate buffer were brought to 20 mM Tris-HCl buffer pH 8.2. **b**-chain was treated with 32 mM DL-dithiothreitol (DTT). A complete carbonmonoxy atmosphere was maintained for Fe-containing chains. Metallated **a**- and **b**-chains were mixed in the ratio 1 : 1.2 at 0°C and stirred for 2 h. The hybrid thus formed was passed through Sephadex G25 (Fine) in 20 mM Tris-HCl buffer pH 7.2 and then through DE23 Cellulose (Whatmann) and CM23 Cellulose (Whatmann), both in 20 mM Tris-HCl buffer pH 7.2. The sample collected sample concentrated by ultrafiltration and stored in liquid nitrogen.

2.2 UV-Vis measurements

Visible spectra were obtained using a double beam Varian Cary 05E spectrophotometer interfaced with an IBM Pentium computer. Spectra were run in the 250–650 nm regions. All UV-Vis spectral studies were carried out at ambient temperature (~23°C) with 100 μ M hybrid Hb solutions in 20 μ M Tris-HCl buffer pH 7.2.

2.3 -SH reactivity study

The reactivity of free -SH groups with 4,4'-dithiodipyridine (4-PDS) was monitored spectrophotometrically at 324 nm as the appearance of 4-thiopyridone.²⁴ A standard solution of 4-PDS was prepared as follows: 50 mg of 4-PDS was transferred to a 50-ml beaker, dissolved in isotonic sodium chloride solution (0.15M) at 60°C, cooled and made up to 50 ml. Exactly 2.5 ml of the hybrid solution (7 μ M, tetramer) in 20 mM Tris-HCl buffer 7.2 was placed in a quartz cuvette. 500 μ l of 4-PDS (4.5 mM) was added to the Hb solution and mixed thoroughly, and the reaction was monitored by measuring the increase in absorbance at 324 nm. The dead time of the reaction was 2 s.

2.4 EPR measurements

EPR measurements were carried out on a Varian E-112 EPR spectrometer operating with 100 kHz field modulation and phase-sensitive detection to obtain the first derivative signal. For X-band work, a multipurpose Varian TE₁₀₂ rectangular cavity was employed. All measurements were performed at 77 K by placing the samples in a cylindrical liquid nitrogen quartz dewar. The Q-band measurements were done on a Variable temperature set up at 100 K by flowing nitrogen gas through liquid nitrogen using a transfer dewar. A modulation amplitude of 5 G, with 10 mW power, time constant of 64 millisecond and scan time of 4 min were used uniformly. DPPH was used as a g-marker.

3. Results

3.1 UV-visible spectra of hybrid hemoglobins

Figure 1 shows the visible spectra of the hybrid Hbs under study. The visible spectra of all hybrid Hbs exhibit split Soret bands, one occurring around

400 nm and the other around 420 nm. The shorter wavelength band (400 nm) is associated with the M²⁺PPIX being 4-coordinated, while the longer wavelength band (420 nm) is associated with a 5-coordinated M²⁺PPIX complex, with the metal ion covalently bonded to the Ne-His (F8).^{17,25} The exact peak positions of the Soret and Q-band (visible) region for these hybrid Hbs are given in table 1 along with those of copper and nickel-reconstituted hemoglobins. The Soret bands of all the tetrameric Hbs under study were deconvoluted for the presence of 4- and 5-coordinated species. Baseline corrections were properly made for all the Hb samples during deconvolution. The deconvolution gives information on the peak position, peak height, half-width at half maximum and integrated intensity for the two species (table 2). From the table it is clear that the ratio of integrated intensity of the 5- to 4-coordinated species was found to be in the following order (series 1):

$$\text{CuHb} < \text{NiHb} < \mathbf{a}_2(\text{Cu})\text{-}\mathbf{b}_2(\text{Ni}) < \mathbf{a}_2(\text{Ni})_2\text{-}\mathbf{b}_2(\text{Cu}) < \mathbf{a}_2(\text{Cu})\text{-}\mathbf{b}_2(\text{FeCO}) < \text{HbCO} < \mathbf{a}_2(\text{FeCO})\mathbf{b}_2(\text{Cu}), \quad (1)$$

with 4-coordination in CuHb and 5-coordination in $\mathbf{a}_2(\text{FeCO})\text{-}\mathbf{b}_2(\text{Cu})$.

Alkaline Bohr effect exhibited by hybrid Hbs has been studied extensively by the use of various methodologies such as, optical studies,²⁰ EPR,³ NMR¹² and transient Raman.¹⁰ $\mathbf{a}_2(\text{Ni})\text{-}\mathbf{b}_2(\text{Fe-CO})$ hybrid hemoglobin exhibits alkaline Bohr effect. The absorption spectra of $\mathbf{a}_2(\text{Ni})\text{-}\mathbf{b}_2(\text{Fe-CO})$ hybrid Hb show marked pH dependence.²⁰ The pH-dependent Soret band positions of this hybrid were deconvoluted and it is found that the ratio of 5- to 4-coordination increases as the pH is raised from 6.5 to 8.5 (table 3). When the visible spectra of $\mathbf{a}_2(\text{Ni})\text{-}\mathbf{b}_2(\text{Fe-CO})$ and $\mathbf{a}_2(\text{Ni})\text{-}\mathbf{b}_2(\text{Fe-O}_2)$ are compared (fig-

Table 1. The Soret and Q-band maxima in reconstituted and hybrid Hbs.

Reconstituted/ hybrid Hb's	Soret band	Q-band
CuHb	404, 417	540, 575
NiHb	399, 420	526, 558, 576
$\mathbf{a}_2(\text{Cu})\text{-}\mathbf{b}_2(\text{Ni})$	403, 419	542, 558, 571
$\mathbf{a}_2(\text{Ni})\text{-}\mathbf{b}_2(\text{Cu})$	401, 419	544, 558, 577
$\mathbf{a}_2(\text{Ni})\text{-}\mathbf{b}_2(\text{FeCO})$	400, 420	541, 558, 575
$\mathbf{a}_2(\text{Cu})\text{-}\mathbf{b}_2(\text{FeCO})$	405, 419	541, 574
$\mathbf{a}_2(\text{FeCO})\text{-}\mathbf{b}_2(\text{Cu})$	397, 419	543, 575

All band positions are in nanometres

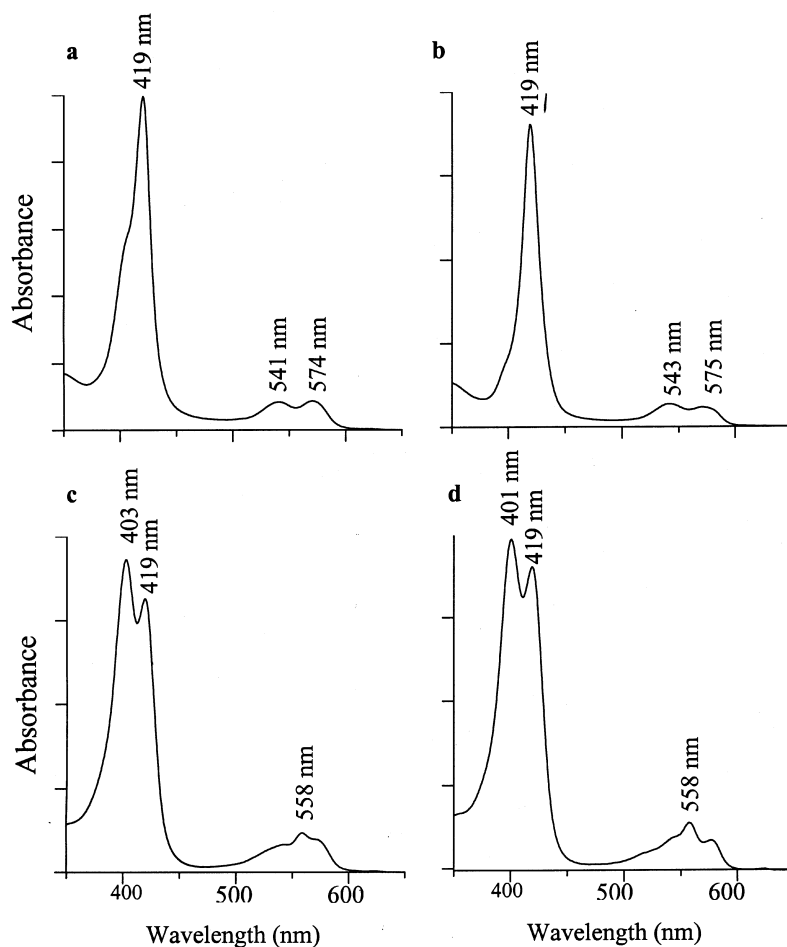


Figure 1. Visible spectra of hybrid Hbs showing the Soret as well as the Q-band regions. (a) $a_2(\text{Cu})-b_2(\text{FeCO})$, (b) $a_2(\text{FeCO})-b_2(\text{Cu})$, (c) $a_2(\text{Cu})-b_2(\text{Ni})$, (d) $a_2(\text{Ni})-b_2(\text{Cu})$.

Table 2. Soret band deconvolution results of reconstituted and hybrid Hbs.

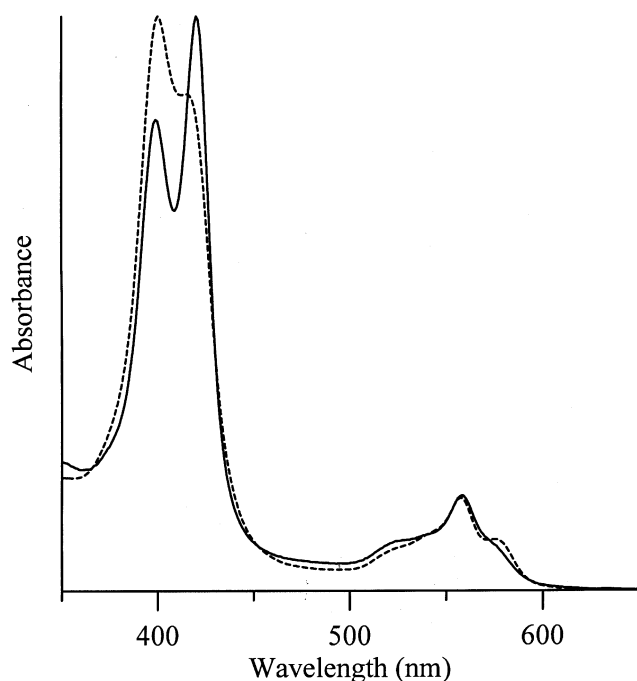
Hb sample	Peak centre (cm^{-1})	Half width (cm^{-1})	Peak height	Integrated intensity	Ratio of area of 5-coord. to 4-coord.
CuHb	23646.57 ^a	466.96	0.149	118.78	0.305
	24730.34 ^b	805.56	0.284	389.43	
NiHb	23745.66 ^a	537.96	0.717	655.51	0.59
	25077.64 ^b	716.84	0.914	1113.76	
$a_2(\text{Cu})-b_2(\text{Ni})$	23735.31 ^a	500.68	0.439	374.13	0.64
	24848.38 ^b	715.61	0.478	582.02	
$a_2(\text{Ni})-b_2(\text{Cu})$	23744.38 ^a	578.82	0.108	106.66	0.66
	24957.78 ^b	797.92	0.119	162.16	
$a_2(\text{Ni})-b_2(\text{FeCO})$	23780.02 ^a	500.99	0.0782	66.58	0.9497
	25026.68 ^b	721.22	0.0572	70.10	
$a_2(\text{Cu})-b_2(\text{Fe-CO})$	23762.12 ^a	480.91	0.370	302.98	1.70
	24658.14 ^b	646.18	0.162	177.73	
FeHb(CO)	23825.56 ^a	469.99	1.1513	919.93	4.01
	24650.04 ^b	739.18	0.1824	229.27	
$a_2(\text{Fe-CO})-b_2(\text{Cu})$	23832.1 ^a	568.20	1.2271	1185.40	6.30
	25010.63 ^b	674.55	0.1640	188.15	

^a5-Coordinated species; ^b4-coordinated species

Table 3. Soret band deconvolution results of $a_2(\text{Ni})\text{-}b_2(\text{FeCO})$ hybrid Hb at 3 different pH's and $a_2(\text{Ni})\text{-}b_2(\text{FeO}_2)$ hybrid Hb.

Hybrid Hb	pH	Peak centre (cm ⁻¹)	Half width (cm ⁻¹)	Peak height	Intensity integrated	Ratio of area of 5-coord. to 4-coord.
$a_2(\text{Ni})\text{-}b_2(\text{FeCO})$	6.5	23780.02 ^a	500.99	0.0782	66.58	0.5686
		25026.68 ^b	721.22	0.0572	70.10	
	7.2	23780.02 ^a	500.99	0.0782	66.58	0.9497
		25026.68 ^b	721.22	0.0572	70.10	
	8.5	23770.82 ^a	499.40	0.9877	838.56	1.5189
		24976.51 ^b	758.94	0.4279	552.06	
$a_2(\text{Ni})\text{-}b_2(\text{FeO}_2)$	7.2	23838.02 ^a	642.33	0.4336	473.44	0.6865
		25011.33 ^b	758.91	0.5345	689.59	

^a5-Coordinated species; ^b4-coordinated species

**Figure 2.** Comparison of the visible spectra of $a_2(\text{Ni})\text{-}b_2(\text{FeCO})$ (solid line) and $a_2(\text{Ni})\text{-}b_2(\text{FeO}_2)$ (dashed line) in 20 mM Tris-HCl pH 7.2.

ure 2), by deconvoluting their Soret bands, it is found that the carbonmonoxy derivative has a higher ratio of integrated intensities of 5- to 4-coordination than the oxy derivative (table 3).

3.2 Sulphydryl reactivity study

When -SH reactivity studies were performed for these hybrid and reconstituted Hbs it was realized that there is a one-to-one correspondence between

our deconvolution result and the -SH reactivity profile. CuHb, which has the lowest ratio of integrated intensity of 5- to 4-coordinated species, showed the lowest reactivity and the $a_2(\text{FeCO})\text{-}b_2(\text{Cu})$ hybrid, the which has maximum ratio, showed the highest reactivity. All the other hybrid Hbs exhibited a reactivity profile in between these two extreme cases (figure 3). Since the -SH reactivity profiles of $a_2(\text{Cu})\text{-}b_2(\text{Ni})$ and $a_2(\text{Ni})\text{-}b_2(\text{Cu})$ are close to NiHb (a representative of T-state Hb) these two hybrids can be termed T-state hybrids. On the other hand, the -SH reactivity profiles of $a_2(\text{Cu})\text{-}b_2(\text{Fe-CO})$ and its complimentary hybrid $a_2(\text{Fe-CO})\text{-}b_2(\text{Cu})$ are comparable to that of HbCO, hence these hybrid Hbs can be termed R-state hybrids.

-SH group reactivity study was conducted on $a_2(\text{Ni})\text{-}b_2(\text{Fe-CO})$ hybrid Hb at three pH values, 6.5, 7.2 and 8.5 (figure 4) and it was found that the reactivity profile increases as the pH is raised from 6.5. Similarly, the sulphhydryl reactivity of $a_2(\text{Ni})\text{-}b_2(\text{Fe-O}_2)$ hybrid Hb was also measured and compared with that of $a_2(\text{Ni})\text{-}b_2(\text{Fe-CO})$ at pH 7.2. It was found that the carbonmonoxy derivative showed higher reactivity than the oxy derivative (figure 5).

3.3 EPR measurements

The paramagnetic copper(II) centre has been effectively used to decipher the type of coordination found in $a_2(\text{Cu})\text{-}b_2(\text{FeCO})$, $a_2(\text{FeCO})\text{-}b_2(\text{Cu})$ (*R-state hybrids*), $a_2(\text{Cu})\text{-}b_2(\text{Ni})$ and $a_2(\text{Ni})\text{-}b_2(\text{Cu})$ hybrid Hbs (*T-state hybrids*). The X-band EPR spectra of these hybrid Hbs are complex due to two reasons: (i) the parallel and the perpendicular lines merge together making the analysis complex; (ii) the hybrid Hbs

contained Cu(II) ion with natural isotopic abundance of ^{63}Cu and ^{65}Cu . The first point of complexity was circumvented by recording the EPR at higher frequency, i.e., at Q-band frequency. The second point was taken care of during simulation of the Q-band EPR spectrum by the inclusion of isotopic compensation and their change in magnetic moments.

In the EPR spectra of all these four hybrid Hbs recorded at Q-band fields, the parallel lines completely separated out from the perpendicular features and contain two sets of four lines partially superimposed (figures 6a, b, 7 and 8). This indicates the presence of two different copper ion environments,

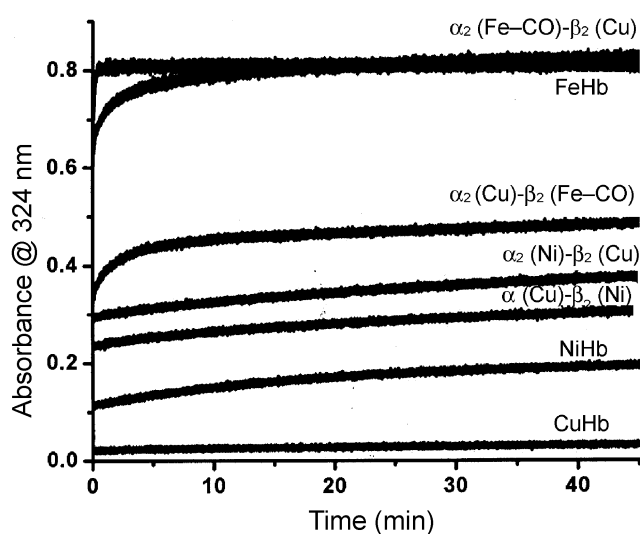


Figure 3. Reactivity profile of the sulphhydryl group of normal, reconstituted and hybrid Hbs towards 4-PDS.

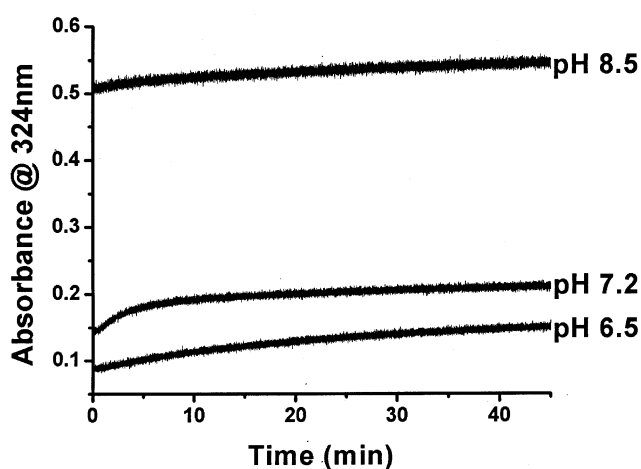


Figure 4. Reactivity profile of the sulphhydryl group of $\alpha_2(\text{Ni})\text{-}\beta_2(\text{FeCO})$ hybrid Hb at three different pH values towards 4-PDS.

namely, 4-coordinated M^{2+}PPIX and 5-coordinated M^{2+}PPIX for all these hybrid Hbs with differing intensity ratios. The perpendicular features of these hybrid Hbs having two components, one with distinctly narrowed superhyperfine lines and another with broadened unresolved superhyperfine structure, again indicates that the Cu(II) ions in both these hybrid Hbs possess of two different metal ion environments.

Though reasonable EPR parameters can be obtained from parallel component, computer simulations were needed to obtain the perpendicular components and the relative amounts of species with reasonable accuracy using the Hamiltonian,

$$H = g_{\parallel} \mathbf{b} B_z S_z + g_{\perp} \mathbf{b} (B_x S_x + B_y S_y) + A_{\parallel} S_z I_z + A_{\perp} (S_x I_x + S_y I_y) + Q' [I_z - 3I(I+1)] + \sum S A_N I^N. \quad (2)$$

The parameters for the 5-coordinated species 1 and 4-coordinated species 2 were obtained from earlier work of Manoharan and co-workers.¹⁷ A comparison of the experimental and the simulated spectra of the R-state hybrid Hbs for the perpendicular regions are given in figures 7 and 8. In the case of 'R'-state hybrid Hb, the best match between the observed and simulated spectra of $\alpha_2(\text{Cu})\text{-}\beta_2(\text{FeCO})$ hybrid Hb was obtained when species 1 and 2 were combined in the ratio of 40 : 60; whereas this ratio for $\alpha_2(\text{FeCO})\text{-}\beta_2(\text{Cu})$ hybrid Hb was 75 : 25. In the case of 'T'-state hybrid Hb, the best fit for $\alpha_2(\text{Cu})\text{-}\beta_2(\text{Ni})$ was obtained when species 1 and 2 were combined in the percentage ratio of 40 : 60; whereas the same

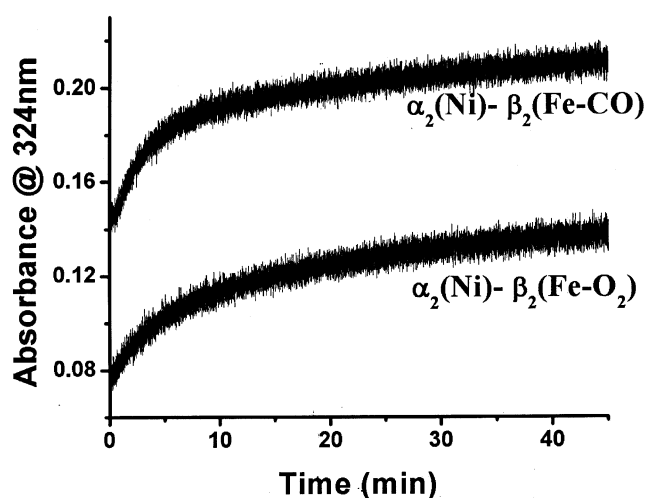


Figure 5. Comparison of the reactivity profiles of the sulphhydryl group of $\alpha_2(\text{Ni})\text{-}\beta_2(\text{FeCO})$ hybrid Hb and $\alpha_2(\text{Ni})\text{-}\beta_2(\text{FeO}_2)$ towards 4-PDS.

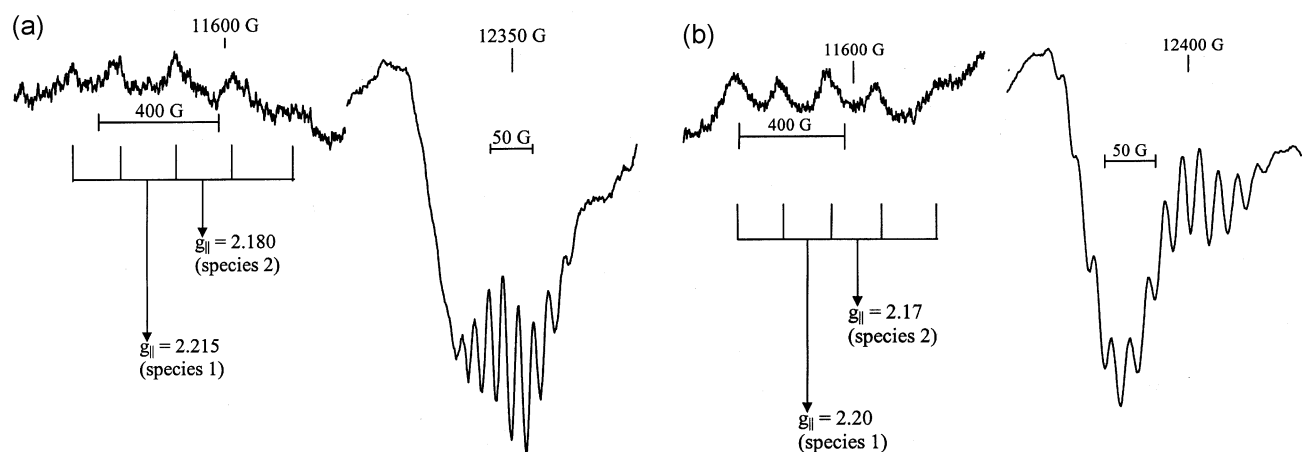


Figure 6. Q-band EPR spectra of hybrid Hbs in 20 mM Tris-HCl buffer pH 7.2 showing the parallel as well as the perpendicular regions recorded at 90 K. (a) $a_2(\text{Cu})-b_2(\text{Ni})$, (b) $a_2(\text{Ni})-b_2(\text{Cu})$.

Table 4. Comparison of EPR spectral parameters of $a_2(\text{Cu})-b_2(\text{FeCO})$, $a_2(\text{FeCO})-b_2(\text{Cu})$, $a_2(\text{Cu})-b_2(\text{Ni})$, $a_2(\text{Ni})-b_2(\text{Cu})$, CuHb and Cu(II) porphyrin complexes.

Reconstituted/hybrid Hb		g_{\parallel}	g_{\perp}	A_{\parallel}^* (Cu)	A_{\perp}^* (Cu)	A_{\parallel}^* (N)	A_{\perp}^* (N)
$a_2(\text{Cu})-b_2(\text{FeCO})$	Species 1 (40%)	2.210	2.044	178.8	11.7	14.6	14.4
	Species 2 (60%)	2.176	2.035	191.0	20.0	14.6	19.1
$a_2(\text{FeCO})-b_2(\text{Cu})$	Species 1 (75%)	2.218	2.048	182.0	14.7	14.6	14.4
	Species 2 (25%)	2.179	2.040	191.0	19.1	14.6	18.8
$a_2(\text{Cu})-b_2(\text{Ni})$	Species 1 (40%)	2.215	2.045	177.0	12.7	14.6	14.3
	Species 2 (60%)	2.180	2.040	210.0	19.8	16.6	18.4
$a_2(\text{Ni})-b_2(\text{Cu})$	Species 1 (60%)	2.208	2.037	182.0	14.4	14.6	14.4
	Species 2 (40%)	2.17	2.027	191.0	18.1	14.6	18.8
CuHb ^a	Species 1 (50%)	2.217	2.054	179.3	11.7	16.6	14.4
	Species 2 (50%)	2.178	2.042	193.6	19.8	14.3	16.5
CuMb ^a (with axial ligand)		2.214	2.045	178.5	12.0	14.6	14.4
CuTPP in CHCl_3 ^b (no axial ligand)		2.187	2.032	209.0	31.8	14.4	15.9
CuTPP-1-methyl imidazole ^c (strong axial ligand)		2.225	2.054	186.0	34.2	13.5	14.8

*A values in 10^{-4} cm^{-1} ; ^aref. [17]; ^bref. [29]; ^cref. [28]

for $a_2(\text{Ni})-b_2(\text{Cu})$ hybrid Hb was 60 : 40. Table 4 gives a compilation of the EPR parameters of these hybrids with species 1 and 2 along with those for pure four- and five-coordinated copper(II) porphyrin systems.

3.4 IHP induced quaternary structural changes in $a_2(\text{Cu})-b_2(\text{Ni})$ and $a_2(\text{Ni})-b_2(\text{Cu})$ hybrid Hbs

Earlier studies have shown that addition of IHP induces the rupture of the metal–nitrogen (Ne-His F8) bond in the *a*-subunit but not in the *b*-subunit.¹⁵ This inequivalence among the subunits was reflected in

our experiments on IHP induced quaternary structural changes in $a_2(\text{Cu})-b_2(\text{Ni})$ and $a_2(\text{Ni})-b_2(\text{Cu})$ hybrid Hbs as observed by Q-band EPR spectroscopy.

The Q-band EPR spectrum of IHP-treated $a_2(\text{Cu})-b_2(\text{Ni})$ (data not shown) shows the presence of only 4 parallel lines with g_{\parallel} value of 2.180 and A_{\parallel} value of $210 \times 10^{-4} \text{ cm}^{-1}$ and highly resolved perpendicular lines (this being characteristic of 4-coordinate species) indicating the presence of only a single species, the four-coordinated species of CuPIX. This is in contrast to the observation of two species before the IHP treatment. The Q-band EPR spectra of the IHP-treated $a_2(\text{Ni})-b_2(\text{Cu})$ hybrid, however,

still exhibits the mixed-metal ion coordination behaviour and there is very little difference between the $a_2(\text{Ni})$ - $b_2(\text{Cu})$ spectrum with and without IHP (figure 9). This shows that CuPIX in the b -subunit is unaffected by the addition of IHP, an observation supporting the subunit heterogeneity.

4. Discussion

4.1 Soret band deconvolution

A study of this kind can throw light on two different aspects of the metal-reconstituted and hybrid hemoglobins, one dealing with conformational change and another pertaining to the differing metal ion environment in different conformations. The most interesting thing is the connection between these two aspects, which in effect is crucial for determining the presence of subunit heterogeneity or otherwise.

It is known that HbCO which falls at the right extreme of the 5–4 coordination ratio series (1) is in R conformation, whereas CuHb which falls at the left extreme is representative of T-state conformation.¹⁷ Our deconvolution results also echo the same trend. CuHb, the T-state tetramer, has the lowest ratio of integrated intensity of 5- to 4-coordination whereas, HbCO- the R-state tetramer has a very high ratio. The $a_2(\text{Fe-CO})$ - $b_2(\text{Cu})$ hybrid which has the highest ratio among all hybrids is at the extreme end of R-

state conformation. The rest of the hybrid Hbs which fall in between these two extremes are representative of intermediate R states (R's).

From the deconvoluted data, it is observed that the half width at half maximum of the lower wavelength (4-coordinated) peak is more than that of the higher wavelength (5-coordinated) peak for the entire set of hemoglobins. This observation can be considered proof of the integrity of our deconvolution results because in the 4-coordinated species, the central metal ion in the porphyrin is not covalently linked to the proximal histidine or any other group and so the porphyrin is not rigidly held except for some Van der Waals' contacts between the heme group and the amino acid groups in the peripheral region. So the linewidth associated with the 4-coordinated heme is expected to be greater in view of the loosening of the metal to nitrogen bond leading to its higher motional behaviour. However, the central metal ion of the porphyrin ring in the 5-coordinated species is covalently bonded to the nitrogen atom of the proximal histidine and, hence, the porphyrin ring is arrested from exhibiting any random motion, resulting in smaller line width than that for the 4-coordination situation.

Furthermore, the spectral changes of $a_2(\text{Ni})$ - $b_2(\text{Fe-CO})$ hybrid with pH variation – *alkaline Bohr effect* – are attributable to the change of coordination state of NiPIX in the a -subunit; namely 4-coordinated NiPIX dominates at pH 6.5 and the contribution of 5-coordination increases on raising the pH.²⁰

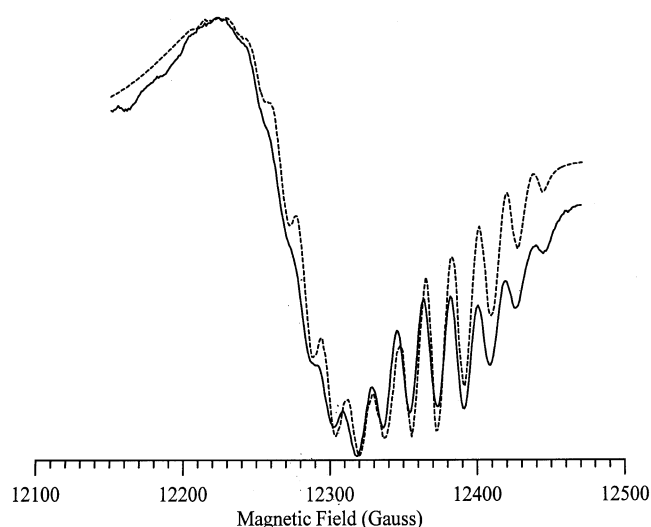


Figure 7. Comparison of the experimental Q-band EPR spectrum (solid line) of $a_2(\text{Cu})$ - $b_2(\text{Fe-CO})$ hybrid Hb and the simulated spectrum (dashed line) due to combination of species 1 and species 2 in the ratio 40:60. Only the perpendicular region is shown.

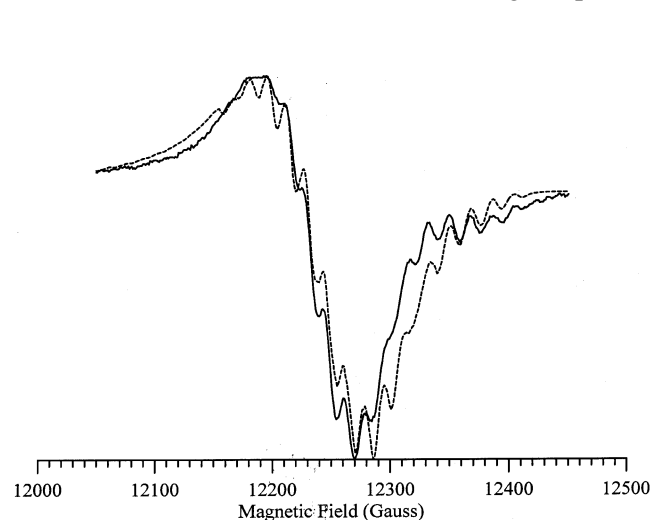


Figure 8. Comparison of the experimental Q-band EPR spectrum (solid line) of $a_2(\text{Fe-CO})$ - $b_2(\text{Cu})$ hybrid Hb and the simulated spectrum (dashed line) due to combination of species 1 and species 2 in the ratio 75:25. Only the perpendicular region is shown.

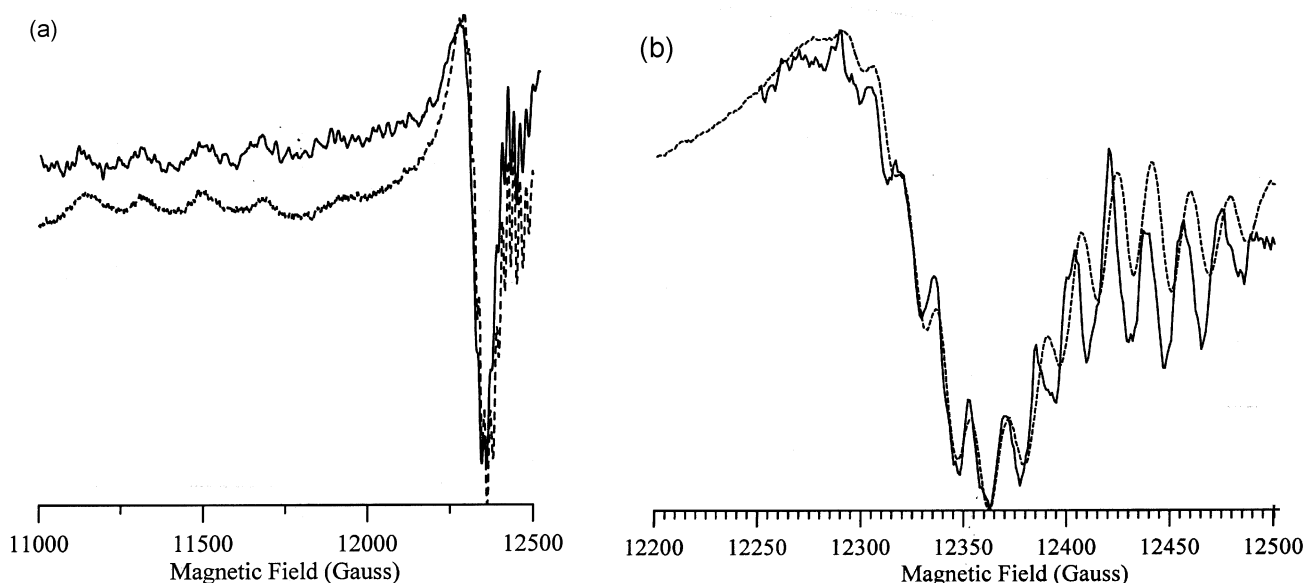


Figure 9. Comparison of the experimental Q-band EPR spectra of $a_2(\text{Ni})\text{-}b_2(\text{Cu})$ hybrid Hb presence (solid line) and absence (dotted line) of IHP. (a) Full region; (b) perpendicular region alone.

The markedly differing intensities of 5- and 4-coordination (figure 2) in the visible spectra of $a_2(\text{Ni})\text{-}b_2(\text{Fe-CO})$ and $a_2(\text{Ni})\text{-}b_2(\text{Fe-O}_2)$ show that the carbonmonoxy derivative is substantially more R-structured than the oxy derivative (table 3). The difference in the visible spectra of $a_2(\text{Ni})\text{-}b_2(\text{Fe-CO})$ and $a_2(\text{Ni})\text{-}b_2(\text{Fe-O}_2)$ hybrid Hbs can be attributed to the fact that complete oxygenation of $a_2(\text{Ni})\text{-}b_2(\text{Fe})$ hybrid under atmospheric oxygen is not possible. It may be recalled that even the K_1 value (dissociation constant for the first oxygen bound) of $a_2(\text{Ni})\text{-}b_2(\text{Fe})$ hybrid is very low at pH 7.2.¹¹

These series of optical spectra of the hybrid Hbs, pH dependence of $a_2(\text{Ni})\text{-}b_2(\text{Fe-CO})$ and a comparison of the oxy and carbonmonoxy derivative of $a_2(\text{Ni})\text{-}b_2(\text{Fe-X})$ (where $X = \text{O}_2/\text{CO}$) clearly bring out the nature of conformational change and their relation to metal ion environment. This derives substantial support both from sulphhydryl reactivity profile experiments as well as EPR.

4.2 Sulphydryl reactivity studies

Cys**93** is located next to the proximal histidine **92**. As the extent of 5-coordination increases, the proximal histidine nitrogen atom is pulled towards the central metal ion of the porphyrin core, and as a result, more room is created around the $-\text{SH}$ group and hence 4-PDS can easily react with the $-\text{SH}$ group and more thiopyridone is evolved, and thus the

higher absorption. Therefore, the Cys **93** group whose reactivity is used as a structural probe in this study reflects also the coordination aspects. The $-\text{SH}$ reactivity profile seen in figure 3 is in complete accord with the 5–4 coordination ratio profile monitored by optical spectroscopy as noted in series (1). CuHb which has a lowest ratio of integrated intensity of 5- to 4-coordinated species shows the lowest reactivity and the $a_2(\text{FeCO})\text{-}b_2(\text{Cu})$ hybrid, the one with the maximum ratio, shows the highest reactivity. It is interesting to note that the $a_2(\text{Fe-CO})\text{-}b_2(\text{Cu})$ hybrid shows a higher reactivity than HbCO. At this point it is necessary to recall the analysis by Makino and Sugita²⁶ on the initial rates of the reaction, which reveal an intermediate, carrying 3 oxygen molecules, that shows a $-\text{SH}$ reactivity even higher than the fully ligated form. In the same way, $a_2(\text{Fe-CO})\text{-}b_2(\text{Cu})$ can be regarded to have a structure which is similar (at the $-\text{SH}$ pocket) to the above intermediate with three oxygen molecules. The reason for the $-\text{SH}$ group of $a_2(\text{Fe-CO})\text{-}b_2(\text{Cu})$ being more reactive than that of HbCO may be attributed to the difference in the ionic radii of the Fe^{2+} and Cu^{2+} . Cu^{2+} being smaller than Fe^{2+} fits comfortably into the cavity of porphyrin, thereby bringing the nitrogen atom of the proximal histidine towards the porphyrin ring more easily than in the case of normal Hb. This in turn creates larger space in the $-\text{SH}$ pocket resulting in higher reactivity for the hybrid than HbCO. It is interesting to note that though the final reactivity of $a_2(\text{Fe-}$

CO)- \mathbf{b}_2 (Cu) is higher than that of HbCO, the initial reactivity of HbCO is higher (as shown by the sharper rise in comparison to the other) than that of \mathbf{a}_2 (Fe-CO)- \mathbf{b}_2 (Cu). This may probably be due to the fact that the heme-heme interaction in the tetrameric HbCO plays a dominant role.

Increasing the pH increases the extent of R character of the hybrid, as clearly illustrated in \mathbf{a}_2 (Ni)- \mathbf{b}_2 (FeCO) hybrid Hb (figure 4). The conformation of the hybrid at pH 6.5 is 'T' as evidenced by the Soret band deconvolution which is equally well reflected in the reactivity of the -SH group of the Cys $\mathbf{b}93$. At higher pH, the reactivity increases as the conformation of the tetramer moves to R. It is also known from the optical studies of Shibayama *et al*²⁰ that the change in the absorption spectra of \mathbf{a}_2 (Ni)- \mathbf{b}_2 (FeCO) hybrid Hb on increase of pH is due to the increase in the 5-coordination behaviour of \mathbf{a} Ni subunit. This behaviour of the \mathbf{a} -subunit must be noted in the context of our earlier explanation that the -SH reactivities of all hybrids are related to the coordination behaviour of the \mathbf{b} -subunit. Now it becomes realistic to say that the M-Ne His(F8) bond in \mathbf{a} -subunit also has a specific role in modulating the ligand affinity and thereby in triggering the allosteric transition, as was suggested by Fujii *et al*²⁷. Based on the increase in the reactivity of -SH group on increasing the pH of \mathbf{a}_2 (Ni)- \mathbf{b}_2 (FeCO) hybrid Hb, it can be concluded that the increase in the 5-coordination behaviour in \mathbf{a} Ni subunit, due to subunit interaction, pushes the \mathbf{b} -Fe subunit to assume stronger 5-coordination behaviour which in effect changes the tertiary structure at the Cys $\mathbf{b}93$ residue. The latter causes an increase in the PDS reactivity. It is also supported by the increase in 5- to 4-coordination ratio monitored by optical spectroscopy. In other words, the establishment of M-Ne covalent bond in the \mathbf{a} -subunit from its dominantly 4-coordinate structure in T conformation is responsible for T \rightarrow R transition. However, the Fe-His bond in \mathbf{a} and \mathbf{b} -subunits are found to behave differently in different subunits. More support for all these observations and inferences come from EPR results.

4.3 EPR of R-state hybrid

The observations by EPR spectroscopy are equally interesting and informative. As has been earlier predicted by Manoharan *et al*,¹⁷ the presence of CuPIX in most tetrameric Hb gives rise to two different metal ion environments. Species 1 is characterized

by higher g_{\parallel} , lower A_{\parallel} (Cu) and not so well resolved perpendicular component. On the other hand, species 2 is characterized by lower g_{\parallel} , higher A_{\parallel} (Cu) and a well-resolved perpendicular component due to the hyperfine lines from ^{63,65}Cu and ¹⁴N. Hence, species 1 basically is a result of 5-coordination with a ruffled porphyrin²⁸ and species 2 is an almost planar 4 coordination site²⁹ (see table 4). We have used these basic EPR structure to understand the Cu-containing sites after simulation in hybrid Hbs.

A comparison of \mathbf{a}_2 (Cu)- \mathbf{b}_2 (FeCO) and its counterpart \mathbf{a}_2 (FeCO)- \mathbf{b}_2 (Cu) hybrid reveal 40 : 60 ratio of species 1 and 2 for the former and 75 : 25 ratio for the latter hybrid. This is in excellent accord with similar trends in the ratio of 5- to 4-coordination from optical spectroscopy (table 2) as well as in the conformational trend measured by -SH reactivity (figure 3). The presence of both 5- and 4-coordination (species 1 and 2) in \mathbf{a} -subunit of \mathbf{a}_2 (Cu)- \mathbf{b}_2 (FeCO) hybrid indicates the presence of different metal ion environments within the same subunit. On the other hand, the enormous increase in 5-coordination of its counterpart, viz., \mathbf{a}_2 (FeCO)- \mathbf{b}_2 (Cu) hybrid is not only because of the inherent presence of Cu in \mathbf{b} -subunit with strong metal-Ne bond but also because of the push given by the 5-coordinated \mathbf{a} -Fe subunit.²⁷

4.4 EPR of T-state hybrid and CuHb

The best fit for \mathbf{a}_2 (Cu)- \mathbf{b}_2 (Ni) and its complimentary hybrid \mathbf{a}_2 (Ni)- \mathbf{b}_2 (Cu) give the 1st and 2nd species ratio as 40 : 60 and 60 : 40 respectively. The presence of species 1 and 2 within the same subunit is indicative of a dynamical process involving 4- and 5-coordination. It is also in accordance with the conformational change by -SH reactivity profile. Above all, the observation of 1 : 1 combination of species 1 and 2 in the EPR of T-state CuHb indicates¹⁷ that this is nothing but a result of dynamics (and hence sum) observed at the individual subunits. It is, therefore, inferred that metal-Ne bond undergoes dynamics both in α and \mathbf{b} -subunits but the 5-coordination is dominant in the \mathbf{b} -subunit as against 4- in \mathbf{a} -subunit. Hence, we should not consider the coordination behaviour exclusive to any subunit. The presence of two different metal ion environments within the same subunit was also discussed in the R-structured hybrids alone. There is also a rationale behind the conformational difference between two T-structured metal reconstituted Hbs - viz., the T of CuHb is

higher than that of NiHb, specially in relation to **a**-subunit. This is due to the relative electronic structural stabilities of 5-coordination environment around the metal with porphyrin in the equatorial plane and Histidine or any such nitrogen base in the 5th coordination. It is very well known that such 5-coordinated nickel (II) complexes are more stable and more in number than the corresponding Cu (II) systems and hence CuHb has definitely a tendency to have more of 4-coordination and hence to be more T-structured than NiHb. This relative T structure is also reflected in their hybrids namely, $\alpha_2(\text{Cu})\text{-}\beta_2(\text{Ni})$ and $\alpha_2(\text{Ni})\text{-}\beta_2(\text{Cu})$ in their optical spectra and -SH reactivities.

4.5 Supporting evidence for mixed-metal ion coordination from optical data on $\alpha_2(\text{Ni})\text{-}\beta_2(\text{Cu})$ and $\alpha_2(\text{Cu})\text{-}\beta_2(\text{Ni})$ hybrid Hbs

Additional evidence for the presence of species 2, namely the 4-coordinated NiPPIX, in both $\alpha_2(\text{Ni})\text{-}\beta_2(\text{Cu})$ and $\alpha_2(\text{Cu})\text{-}\beta_2(\text{Ni})$ hybrid Hbs comes from the optical spectra of these two hybrids (figure 10), more clearly so from the Q-band (visible) region. The peak at 558 nm is assigned to the four coordinate NiPPIX by Shelnutt *et al.*¹⁸ Both $\alpha_2(\text{Ni})\text{-}\beta_2(\text{Cu})$ and $\alpha_2(\text{Cu})\text{-}\beta_2(\text{Ni})$ hybrid Hbs have a peak at 558 nm indicating the presence of species 2 in both these hybrid Hbs. It is interesting to note that the 558 nm peak in $\alpha_2(\text{Ni})\text{-}\beta_2(\text{Cu})$ is more intense than it is in its

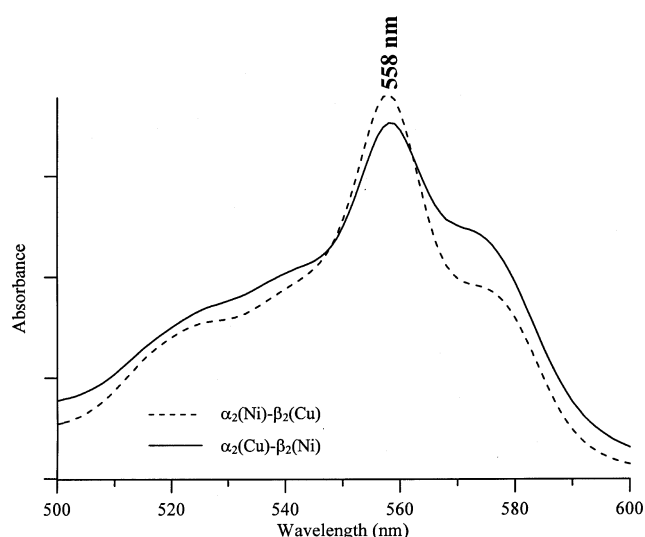


Figure 10. Comparison of Q-band region of the visible spectra of $\alpha_2(\text{Cu})\text{-}\beta_2(\text{Ni})$ and $\alpha_2(\text{Ni})\text{-}\beta_2(\text{Cu})$ hybrid Hbs, both showing peaks at 558 nm.

complementary hybrid $\alpha_2(\text{Cu})\text{-}\beta_2(\text{Ni})$. This in turn supports our Q-band EPR spectral simulation results, which shows that M^{2+}PPIX in the **a**-subunit has 60% of four coordination behaviour, whereas the **b**-subunit has only 40% of four coordination behaviour. This is clearly reflected in our optical spectra of the two hybrid Hbs. The $\alpha_2(\text{Ni})\text{-}\beta_2(\text{Cu})$ hybrid Hb with intense 558 nm peak, has greater amount of 4-coordination behaviour, its complementary hybrid $\alpha_2(\text{Cu})\text{-}\beta_2(\text{Ni})$ hybrid Hb, with less intense 558 nm peak, has lesser amount of 4-coordination behaviour because of the presence of NiPPIX in the **b**-subunit.

Support for the presence of mixed-metal ion coordination in hybrid Hbs also comes from the recent resonance Raman studies on hybrid Hbs by Swarnalatha *et al.*³⁰ Resonance Raman studies were done on both 'T' and 'R' state hybrid Hbs and it was concluded that two different heme environments exist within a similar subunit which is due to the dynamic equilibrium between the 4- and 5-coordination on the hemes with constant "breaking-making" of the M-Ne histidine bond.

A comment on the difference in the optical spectra of $\alpha_2(\text{Ni})\text{-}\beta_2(\text{FeCO})$ and $\alpha_2(\text{Ni})\text{-}\beta_2(\text{FeO}_2)$ hybrids is noteworthy in the light of the work of Fujii *et al.*²⁷ They observed that the first oxygen binding to the **b**-heme may be linked to the metal-proximal histidine interaction in the α -subunits and the reverse effect is minimal. This may be the reason for the lack of complete oxygenation of the **b**-subunit in $\alpha_2(\text{Ni})\text{-}\beta_2(\text{Fe})$. Therefore, the oxy derivative should be rigorously called $[(\alpha^{\text{Ni}}\beta^{\text{Fe}})(\alpha^{\text{Ni}}\beta^{\text{FeO}_2})]$. The proximal histidine interaction with the metal ion in the **a**-subunit, leading to 5-coordination pushes the **b**-heme in such a fashion as to increase the 5- to 4-coordination ratio and hence the conformational push to the R-structure. This is obvious in the case of $\alpha_2(\text{Ni})\text{-}\beta_2(\text{FeCO})$ which has a larger 5- to 4-coordination ratio at higher pH indicating the **a**-Ni site has increased amount of M-Ne interaction. The process of formation of this M-His linkage is hence part of a dynamical process within the same subunit, for which we have provided evidence also through EPR.

Support for mixed-metal ion behaviour in $\alpha_2(\text{Cu})\text{-}\beta_2(\text{FeCO})$ within the same subunit comes from the earlier results on Ni(II)-Fe(II) hybrid Hbs by Shibayama *et al.*¹², who have overlooked the presence of mixed coordination within the **a** and **b**-subunits. In the case of $\alpha_2(\text{Ni})\text{-}\beta_2(\text{FeCO})$, the N_αH signal of the **a**(Ni) subunits is detected at 77 ppm only at high pHs. At pH 7.4, the N_αH resonance markedly reduces

in intensity, and at lower pH or in the presence of IHP, it is difficult to detect. This N_dH resonance occurs as a result of a paramagnetic, 5-coordinated Ni(II). At high pH, since the hybrid is dominated by the 5-coordinated NiPPIX, the N_dH signal is observed at full intensity. Here it must be noted that even at pH 7.2, the observation of N_dH signal due to 5-coordinated NiPPIX, is at reduced intensity. This adds support to our Q-band EPR simulation results on $a_2(Cu)-b_2(FeCO)$ hybrid that at neutral pH, CuPPIX in the **a**-subunit exhibits mixed coordination, a 5-coordinated species with axial ligation coming from the $Ne-HisF8$ and the other without any axial ligation. However, it is necessary to point out that the **a**-subunit always has more 4-coordination with a small amount of 5-coordination character due to mixed-metal ion coordination of proximal histidine prone to motion towards the metal in porphyrin. In other words, the tendency of $Ne-His$ to bond with the metal in the **a**-subunit has the tendency switch "on-off". Since, on an average, $M-Ne$ (His) distance is large, the **a**-subunit heme appears to be 4-coordinated with the possibility of the said bond getting shorter as pH increases. It is the other way for the **b**-subunit even for ions such as Ni(II) and Cu(II) in $M^{2+}PPIX$ where the tendency is greater towards 5-coordination due to generally reduced $M-Ne$ distance. This must also be the reason why we see 1 : 1 of species 1 and 2 distribution in CuHb.¹⁷ Exactly for the same reason, species 2 dominates $a_2(Cu)-b_2(FeCO)$ (which is an intermediate R conformation) and species 1 dominates $a_2(FeCO)-b_2(Cu)$ hybrid Hb (which is in an extreme R conformation).

Support for the mixed-metal ion behaviour in the **b** site of $a_2(FeCO)-b_2(Cu)$, also comes from the earlier results on Ni(II)-Fe(II) hybrid Hbs by Shibayama *et al*¹². The proton NMR spectra of deoxy $a_2(Fe)-b_2(Ni)$ exhibit a resonance at 70.5 ppm which is assigned to the proximal histidyl N_dH protons. Similar measurements were carried out for the half-liganded $a_2(FeCO)-b_2(Ni)$ and it was found that the CO-bound Fe subunits do not show hyperfine-shifted resonances because of diamagnetism of the porphyrin iron. The N_dH resonances of the **b**(Ni) subunits are shifted downfield by approximately 5 ppm upon CO binding to the partner **a**(Fe) subunits at pH 7.4 and pH 8.5, but the resonances are somewhat broader than those of the deoxy $a_2(Fe)-b_2(Ni)$. This broadening could have arisen only because of dynamics slightly faster than the NMR timescale involving the NiPPIX relative to $Ne-His$ induced by subunit interaction during the addition of CO to Fe subunit. This

also adds support to our Q-band EPR simulation results on $a_2(FeCO)-b_2(Cu)$ hybrid that at neutral pH, CuPPIX in the **b**-subunit exhibits mixed coordination, a 5-coordinated species with axial ligation coming from the $Ne-HisF8$ and the other without any axial ligation. Similar effects are also observed in $a_2(Ni)-b_2(Cu)$ hybrid Hb at pH 8.5. However, the absence of NMR signal for N_dH resonances of the **a**-Ni in the T-structured deoxy $a_2(Ni)-b_2(Fe)$ and also in NiHb is perplexing! It is, however, possible that Ni in the **a**-subunit, having only two electrons for providing paramagnetism as compared to 4 in iron, lesser extent of 5-coordination and greater dynamics between 4- and 5-coordination, must have shifted to lower ppm and broadened beyond detection.

5. Conclusion

In summary, hybrid Hbs, based on their reactivity towards 4-PDS, have been classified as R-state or T-state, or R (intermediate) when they show an intermediate reactivity. There exists some correlation between conformational change and coordination behaviour. The same correlation is also observed for hybrids exhibiting the alkaline Bohr effect and for such hybrids having FeCO or FeO₂ as one of the constituents. The Q-band EPR spectral studies on Cu(II) containing R- and T-state hybrid Hbs and subsequent simulation of the resulting spectra reveals the presence of two different metal ion environments for CuPPIX within both the **a**- and **b**-subunits but in varying percentage compositions. All hybrids point to the presence of mixed-metal ion coordination in both subunits and question the acceptance of subunit heterogeneity. In addition, the observation of Fujii and co-workers²⁷ that the $M-Ne$ His (F8) bond in the **a**-subunit has also a role in modulating the ligand affinity and thereby triggering the allosteric transition just like the counterpart in **b**-subunit, is confirmed by our work. All these are possible only if there is a dynamics of motion between 5- and 4-coordination in all the subunits.

Acknowledgements

PTM thanks the Department of Science and Technology, Govt. of India for financial support and SR and SV the Council of Scientific and Industrial Research, New Delhi for fellowships. PTM also thanks the Jawaharlal Nehru Centre for Advanced Scientific Research, Bangalore for the Honorary Professorship.

References

1. Ackers G K and Smith F T 1987 *Annu. Rev. Biophys. Chem.* **16** 583
2. Ogawa S and Shulman R G 1972 *J. Mol. Biol.* **70** 315
3. Ikeda-Saito M, Yamamoto H and Yonetani T 1977 *J. Biol. Chem.* **252** 8639
4. Miura S and Ho C 1982 *Biochemistry* **21** 6280
5. Miura S and Ho C 1984 *Biochemistry* **23** 2492
6. Perutz M F 1972 *Nature (London)* **237** 495
7. Perutz M F, Fersht A R, Simon S R and Roberts G C K 1974 *Biochemistry* **13** 2174
8. Perutz M F, Kilmartin J V, Nagai K, Szabo A and Simon S R 1976 *Biochemistry* **15** 378
9. Inubushi T and Yonetani T 1983 *Biochemistry* **22** 1894
10. Scott T W, Friedman J M, Ikeda-Saito M and Yonetani T 1983 *FEBS Lett.* **158** 68
11. Shibayama N and Morimoto H 1986 *J. Mol. Biol.* **192** 331
12. Shibayama N, Inubushi T, Morimoto H and Yonetani T 1987 *Biochemistry* **26** 2194
13. Ishimori K and Morishima I 1988 *Biochemistry* **27** 4060
14. Nagai K and Kitagawa T 1980 *Proc. Natl. Acad. Sci. (USA)* **77** 2033
15. Maxwell J C and Caughey W S 1976 *Biochemistry* **15** 388
16. Manoharan P T, Alston K and Rifkind J M 1985 in *Biological & inorganic copper chemistry* (eds) K D Karlin and J Zubieta (New York: Adeinine Press)
17. Manoharan P T, Alston K and Rifkind J M 1986 *J. Am. Chem. Soc.* **108** 7095
18. Shelnut J A, Alston K, Ho J-Y, Yu N-T, Yamamoto T and Rifkind J M 1986 *Biochemistry* **25** 620
19. Shibayama N, Ikeda-Saito M, Hori H, Itaroku K, Morimoto H and Saigo S 1995 *FEBS Lett.* **372** 126
20. Shibayama N, Morimoto H and Miyazaki G 1986 *J. Mol. Biol.* **192** 323
21. Kilmartin J V, Fogg J, Luzzana M and Rossi-Barnerdi L 1973 *J. Biol. Chem.* **248** 7039
22. Geraci G, Parkhurst L J and Gibson Q H 1969 *J. Biol. Chem.* **244** 4664
23. Rossi-Fanelli A, Antonini E and Caputo A 1958 *Biochim. Biophys. Acta* **30** 608
24. Ampulski R S, Ayers V E and Morell S A 1967 *Anal. Biochem* **32** 163
25. McLees B D and Caughey W S 1969 *Biochemistry* **7** 642
26. Makino N and Sugita Y 1982 *J. Biol. Chem.* **257** 163
27. Fujii M, Hori H, Miyazaki G, Morimoto H and Yonetani T 1993 *J. Biol. Chem.* **268** 15386
28. Alston K and Storm C B 1979 *Biochemistry* **79** 4292
29. Manoharan P T and Rogers M T 1969 in *ESR of metal complexes* (ed.) T F Yen (New York: Plenum Press) p. 143
30. Venkatesh Rao V, Balakrishnan G and Manoharan P T 2002 *Biopolymers* **67** 156